doi:10.2533/chimia.2019.707 Chimia 73 (2019) 707–713

Catalyst Development for Water/CO_2 Co-electrolysis

Abhijit Dutta[a§], Francesco Bizzotto[a§], Jonathan Quinson[b], Alessandro Zana[a], Carina Elisabeth Morstein[a], Motiar Rahaman[a], Alena Cedeño López[a], Matthias Arenz[a*], and Peter Broekmann[a*]

Abstract: Herein, we discuss recent research activities on the electrochemical water/CO_2 co-electrolysis at the Department of Chemistry and Biochemistry of the University of Bern (Arenz and Broekmann research groups). For the electrochemical conversion of the greenhouse gas CO_2 into products of higher value catalysts for two half-cell reactions need to be developed, *i.e.* catalysts for the reductive conversion of CO_2 (CO_2RR) as well as catalysts for the oxidative splitting of water (OER: Oxygen Evolution Reaction). In research, the catalysts are often investigated independently of each other as they can later easily be combined in a technical electrolysis cell. CO_2RR catalysts consist of abundant materials such as copper and silver and thus mainly the product selectivity of the respective catalyst is in focus of the investigation. In contrast to that, OER catalysts (in acidic conditions) mainly consist of precious metals, *e.g.* Ir, and therefore the minimization of the catalytic current per gram Ir is of fundamental importance.

Keywords: Ag foam · CO_2RR · Ir NPs catalyst · OER

Dr. Abhijit Dutta received his PhD in chemistry from the Indian Institute of Engineering Science and Technology, Shibpur (2012). He worked as post-doctoral fellow at the National University of Singapore. Currently, he works as a post-doctoral researcher in Peter Broekmann's research group at the University of Bern. His current research focuses on the development of various *operando* spectroscopies to characterize novel electrocatalysts for the selective conversion of CO_2 to value-added products.

Francesco Bizzotto studied technical chemistry at the University of Padua (Italy) and received his MSc in 2014 after a period as visiting student at Åbo Akademi (Finland). After a short experience in industry, he joined in 2016 the group of Matthias Arenz at the University of Bern and received his PhD in 2019. His main research interests focus on the investigation of the fundamental properties of single crystals and nanostructured model catalysts for the oxygen evolution reaction (OER).

Dr. Jonathan Quinson did his undergraduate studies at ESPCI ParisTech, France where he also received a MSc degree. He holds a Master of Research degree in Green Chemistry: Energy and the Environment from Imperial College London (UK). He received his PhD from the University of Oxford (UK) where he worked in-between the Materials and Chemistry departments on synthesis of carbon nanomaterials bio-spectro-electrochemistry before moving to Denmark. At the University of Copenhagen he worked as a Marie Skłodowska-Curie research Fellow on the synthesis of surfactant-free nanoparticles for energy and electrochemical applications.

Carina Elisabeth Morstein obtained her MSc in chemistry (2018) from the University of Bern (Switzerland). For her master thesis she worked on the electrochemical conversion of CO_2 into value-added products, particularly focussing on Ag-based catalysts. In 2019 she started a PhD project on applied nano-tribology at the Karlsruhe Institute of Technology (KIT).

Dr. Alessandro Zana did his PhD work in the group of Matthias Arenz, first at the University of Copenhagen (2011–2016) and later at the University of Bern. He is currently working in the field of electrochemistry/electrocatalysis, interfaces and collective properties of nanoparticles. He is interested in studying electronic properties of nano-systems, developing new solutions for renewable energy sources.

*Correspondence: Prof. P. Broekmann[a]; Prof. M. Arenz[a]
E-mail: peter.broekmann@dcb.unibe.ch; matthias.arenz@dcb.unibe.ch
[a]Department of Chemistry and Biochemistry, University of Bern, Freiestrasse 3, CH-3012 Bern; [b]Department of Chemistry, University of Copenhagen, Universitetsparken 5, Copenhagen 2100 Denmark; [§]Equally contributing first authors

Dr. Motiar Rahaman received his MSc in chemistry (2013) from the Indian Institute of Technology Madras, Chennai. He obtained his PhD (2018) on the electrochemical conversion of CO_2 into value-added products from the University of Bern (group of Peter Broekmann). Currently he works as a post-doctoral fellow at the University of Cambridge (UK).

Alena Cedeño López studied chemistry in Bern (Switzerland). After receiving her MSc (Chemistry and Molecular Sciences) in 2016, she joined the Interfacial Electrochemistry Group of Peter Broekmann as a PhD student. Her PhD project focuses on the preparation and characterization of materials for semiconductor and electrocatalysis applications.

Prof. Dr. Matthias Arenz received his PhD in physical chemistry from the University of Bonn, Germany, in 2002. He worked as post-doctoral Feodor Lynen fellow at the Lawrence Berkeley National Laboratory (LBNL), USA, before starting his independent career with an Emmy Noether Fellowship at the Technical University of Munich, Germany in 2006. In 2010 he was appointed Associate Professor at the University of Copenhagen (Denmark) and in 2016 Professor of Physical Chemistry at the University of Bern (Switzerland). His current research focuses on electrocatalysis for energy conversion, nanoparticle synthesis and experimental method development.

Prof. Dr. Peter Broekmann obtained his MSc in chemistry (1998) and a PhD (2000) from the University of Bonn. After a post-doctoral stay at the University of Twente (The Netherlands) in 2001, he became project leader at the Institute of Physical Chemistry in Bonn. Since 2008 he holds a lecturer position for electrochemistry at the University of Bern (Switzerland). His research focuses on metal deposition processes for semiconductor and electrocatalysis applications.

1. Introduction

The large-scale conversion of the greenhouse gas CO_2 into products of higher value is today considered a technologically feasible approach to mitigate the increase of CO_2 in our atmosphere which has already reached levels of about 410 ppm.[1]

A paradigm shift currently drives both the energy and mobility sectors away from fossil energy sources (coal, oil, and natural gas) towards renewables (hydro, wind, and solar). It is also evident that the chemistry sector has to follow this trend, which will surely affect entire production chains of most commodity and fine chemicals our daily life is based on. This so-called 'energy transition' can therefore be considered as a truly intersectorial challenge which calls for new transsectorial strategies. Several technologies have already been devised to reduce levels of CO_2 in the atmosphere.[2] Among these, CO_2 reduction by electrochemical means deserves particular attention as it can transform CO_2 directly back into synthetic fuels (so-called e-fuels) or other platform chemicals of high value. In particular the electrochemical co-electrolysis of water and CO_2 has the great potential to directly interlink the energy sector to the chemistry sector. A prime example hereof is the so-called Rheticus process which combines an electrochemical conversion of CO_2 into CO, one essential reactant for the subsequent production of butanol and hexanol based on a fermentation approach.[3] The CO_2 reduction reaction might become not only economically feasible in future but also truly sustainable, in particular when the surplus of renewables originating from solar radiation, wind power, and hydro sources is used as energy input for this electrochemical CO_2 conversion. This so-called 'power to value' concept might become one important element among others contributing in future to the closing of the anthropogenic carbon cycle.

This electrocatalytic process typically relies on the oxidative splitting of water (OER: Oxygen Evolution Reaction) and the reductive conversion of CO_2 (CO_2RR: CO_2 Reduction Reaction). Whereas oxygen (O_2) is the only product that can form on the anode side when using aqueous environments, irrespective which anode material is used (*e.g.* IrO_2, RuO_2, or FeNi-based systems), a variety of different CO_2RR products can be produced on the cathode side, ranging from formate, carbon monoxide (CO), saturated and non-saturated hydrocarbons (*e.g.* methane, ethylene)[4] to oxygenates of various chain length and energy density (*e.g.* methanol, ethanol, and n-propanol).[5] It is mainly the chemical nature and the structure/morphology of the electrocatalyst which governs the resulting performance of the water/CO_2 co-electrolysis. In the following we give a short review of our previously published research in this area.

2. Result and Discussion

2.1 *Preparation and Characterization of the Ag-based CO_2RR Catalyst*

Fig. 1 depicts the basic concept of the novel hydrogen template and additive-assisted metal foaming process. This approach has been adopted from the method originally introduced by Shin *et al.* for Cu- and Sn-based systems.[6] The standard plating bath for the Ag foam deposition was composed of 1.5 M H_2SO_4 (prepared from 96% H_2SO_4, ACS grade, Sigma-Aldrich) serving as support-

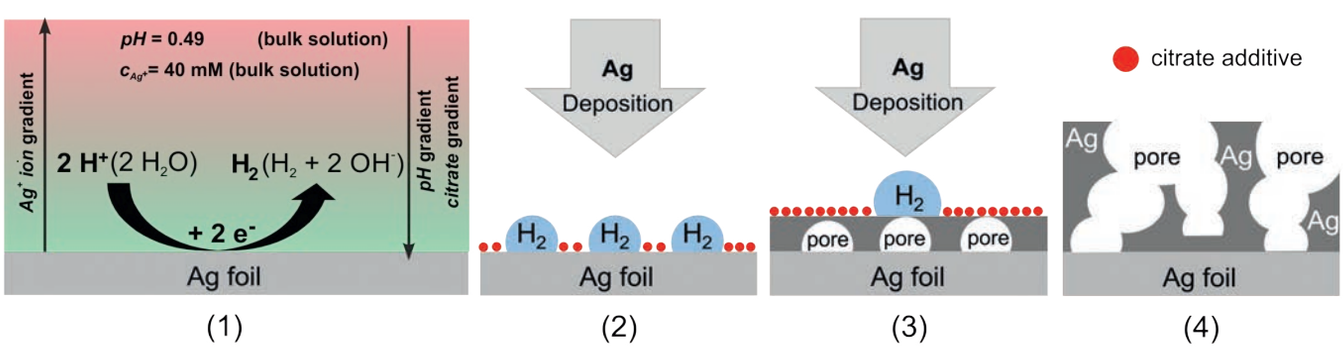

Fig. 1. Scheme demonstrating the basic principle of the template- and additive-assisted metal foam deposition (adopted from ref. [7] with permission from the ACS).

ing electrolyte, 0.02 M Ag_2SO_4 (Sigma Aldrich, purity ≥ 99.5%), and 0.1 M $Na_3C_6H_5O_7$. 2 H_2O (tri-sodium citrate di-hydrate, ACS grade > 99.7%, Merck).[7]

Key to the metal foaming process is the hydrogen evolution reaction (HER) which is superimposed on the primary metal deposition when applying extraordinarily high current densities in the order of several amperes per square centimetre geometric surface area.[6] Under these harsh experimental conditions hydrogen gas bubbles evolve on the electrode and serve as transient geometric templates for the metal foaming process.[8] Sources of the hydrogen evolution reaction (HER) are proton reduction from the acidified aqueous solutions and reductive water splitting. The latter process is inevitably initiated at these high current densities of –3 Acm^{-2} as both the metal deposition and the proton reduction are already mass transport limited under these harsh experimental conditions. Further, both partial HERs lead to substantial changes of the local pH at electrode surface as consequence of the massive H^+ consumption and OH^- production.[7] The local pH turns therefore from strongly acidic to neutral or even alkaline, thus resulting in a pronounced interfacial pH gradient along the surface normal (Fig. 1). Given the pH of 0.49 in the 'bulk' of the Ag plating bath and considering the comparably low acidity of the tribasic citric acid, one can assume that the dissolved citrate anions are nearly quantitatively transformed into citric acid in the bulk solution.[7] As indicated in Fig. 1, the massive HER creates a reactive boundary layer in which several reactions takes place prior to the actual Ag electrodeposition. Due to the pH-dependent deprotonation of the citric acid, an extra gradient of the citrate concentration appears along with the pH gradient (Fig. 1). In this scenario it is the HER which ultimately activates the additive action of the citric acid/citrate at the location where it is actually desired. Furthermore, Ag^+ ions undergo a complexation reaction with the chelating citrate ligands prior to their deposition on the substrate. Given the high current density of J = –3A cm^{-2} and the relatively low Ag^+ concentration of 40 mM in the bulk electrolyte, the Ag deposition becomes readily mass transport limited with an Ag^+ concentration that drops down to zero at the electrode surface. As a consequence, an Ag^+ ion gradient appears under such harsh conditions as further constituent part of such reactive boundary layer (Fig. 1).

Fig. 2 depicts the morphological characteristics of the Ag foam yielded after 20 s of deposition. Compared to the corresponding additive-free deposition process,[7] this Ag foam shows a uniform appearance even on the larger length scale with an open-cell architecture of interconnected macro-pores (panel a and b). However, these macro-pores are significantly smaller than in the case of the citrate-free metal-plating process.[7] This observation can be seen as a clear hint for a citrate-mediated additive action at the interface which affects not only nucleation and growth of the Ag itself, but also the formation and growth of the gaseous H_2-template at the emerging foam. In addition to the primary macro-porosity originated by the gaseous H_2-template, the scaffold of the 3D foam itself is porous, too. The macro-pore sidewalls in Fig. 2 (panel a and b) are composed of randomly distributed needle-like Ag particles of about 400 nm length and diameters below 50 nm. The comparison with the additive-free foaming process[7] demonstrates a clear involvement of the citrate additive in this action which causes such highly anisotropic Ag growth on the nm length scale.

2.2 *Testing of the CO_2RR Performance*

The product distribution of the CO_2RR carried out over the Ag foam electrocatalyst is summarized in Fig. 3 (panel a and b). 1 h CO_2RR screening experiments were carried out in classical half-cell measurements in the potential range from –0.3 V to –1.6 V vs RHE. CO is the main CO_2RR product in the initial potential range starting from –0.3 V and extending to –1.2 V vs RHE. CO formation on the novel Ag foam catalyst sets in at comparably low over-potentials which are ~300 mV less negative as compared to the CO_2RR onset on the polycrystalline Ag foil reference (panel c). The anodically shifted CO_2RR onset over the Ag foam is pointing to an improved catalytic activity and comparable or even superior to the best Ag-based CO forming catalysts reported so far in literature for aqueous environments.[9]

The CO partial current increases from j_{CO} = –0.02 mA cm^{-2} to j_{CO} = –14.72 mA cm^{-2} when going from –0.3 V to –1.2 V vs RHE (panel a). The partial current densities on the Ag foam are about one order of magnitude higher than the Ag foil reference system.[7] This can be rationalized by a convolution of surface area effects and an increased electrocatalytic activity. The FE_{CO} values thereby never fall below 90%. This extended plateau region in the FE_{CO} vs E plot of about ~900 mV is insofar remarkable for aqueous reaction environments as polycrystalline Ag electrocatalysts typically show a peak-like behavior in their FE_{CO} vs E plot regarding the CO formation (panel c). The extended ~900 mV wide plateau in the FE_{CO} vs E plot (panel b) can be regarded as a clear experimental hint for a *CO binding strength that is considerably increased with respect to the polycrystalline Ag foil reference (panel c). CO adsorption is favoured over the competitive H adsorption in particular at those lower overpotentials. The strongly bound *CO thereby serves as an effective suppressor with regard to the HER.

An increased *CO binding strength presumably goes along with an increase in the *CO surface coverage and an extended residence time on the catalyst surface. Both effects are essential for the second characteristic potential regime in the FE_{CO} vs E plot (panel b) that starts at E < –1.1 V vs RHE and involves a drastic drop-down of the FE_{CO} down to 11% at –1.6 V vs RHE accompanied by the simultaneous raise of the FE_{H_2} values up to 64%. Such drastic decrease of the FE_{CO} is typically associated with the

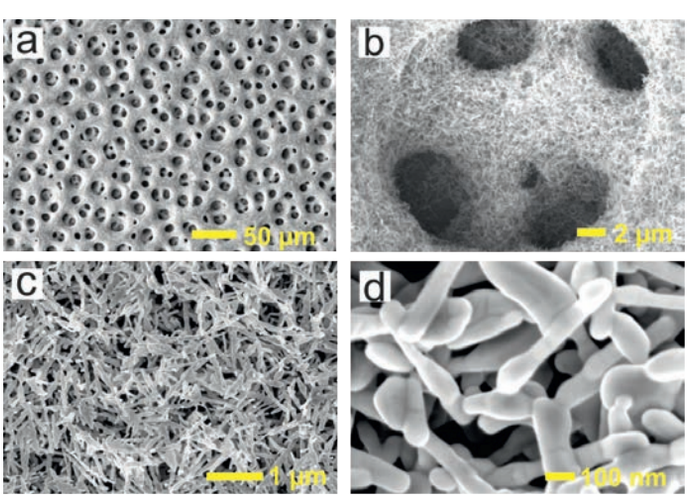

Fig. 2. Morphology of the Ag foam catalyst a) Primary macro-porosity of the foam; b) Individual macro-pore; c) Secondary side-wall porosity; d) Anisotropic Ag particles (adopted from ref. [7] with permission from the ACS).

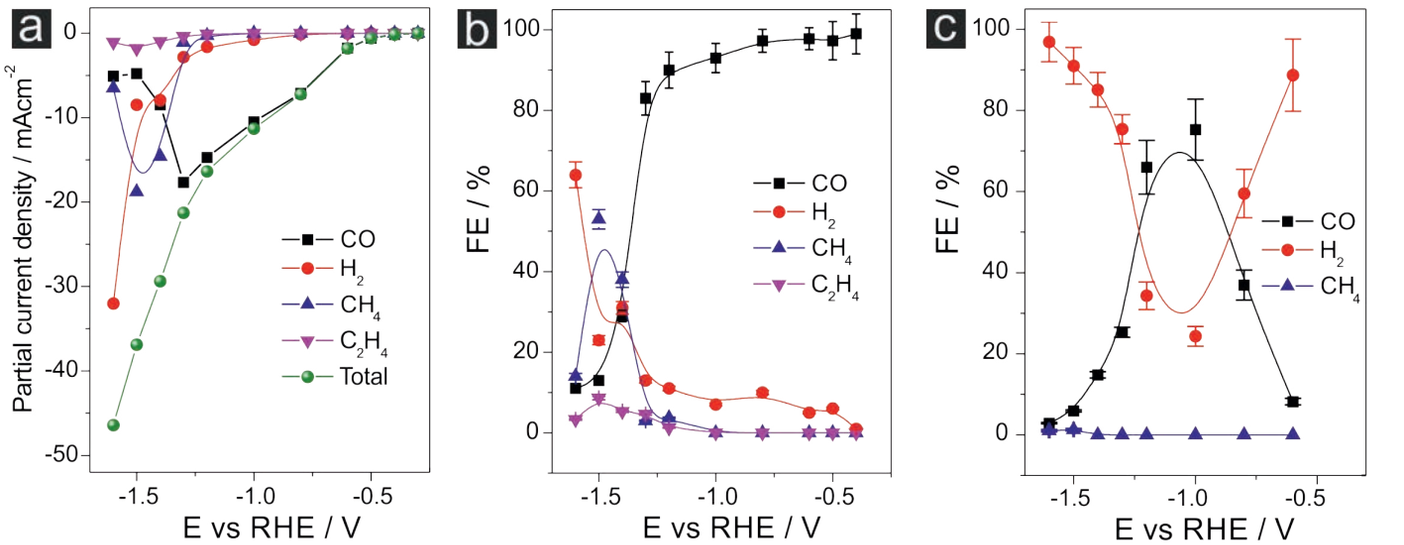

Fig. 3. a) Potential (E) dependent product distribution of the CO_2RR displayed as partial current densities normalized to the geometric surface area (1 h potentiostatic CO_2RR carried out at each potential applied using a freshly prepared Ag foam catalyst); b) Corresponding plot of the Faradaic efficiencies (FEs) as function of the applied electrolysis potential (E); c) Potential (E) dependent product distribution of the CO_2RR on an Ag foil electrode displayed as Faradaic efficiencies (FEs) (adopted from ref. [7] with permission from the ACS).

onset of the CO_2 transport limitation in the course of the CO_2RR at higher reaction rates. A unique feature of the novel Ag foam catalysts, never reported before for any other Ag-based CO_2RR catalyst, concerns the appearance of CH_4 as reaction product. CH_4 formation sets in at E < –1.1 V vs RHE and reaches a maximum in its Faradaic efficiency of remarkable FE_{CH_4} = 51% at –1.5 V vs RHE before it decreases again.

Such high C1 hydrocarbon production rates and efficiencies were reported so far only for Cu-based electrocatalysts[10] whereas Ag was considered as a predominantly CO forming catalyst due to its weak interaction with the formed *CO, which therefore is readily released from the Ag catalyst surface.[11]

Further support for these unique characteristics comes from the intriguing observation that the novel Ag foam catalyst is also capable of C–C coupling reactions (panel a and b). C_2H_4 is formed in the same potential window between –1.1 V and –1.6 V vs RHE with a maximum of $FE_{C_2H_4}$ = 8.6% at –1.5 V vs RHE. The total hydrocarbon efficiency therefore amounts to 59.6% at –1.5 V vs RHE. Also note that such C–C coupling requires the stabilization of the *CO intermediates at the catalyst surface, thus resulting in a sufficiently high surface concentration and mean residence time of *CO as discussed for Cu.[11] Previous XPS inspection of the Ag foam catalyst prior and after ec-CO_2RR could exclude any trace contaminations of Cu as origin of the observed anomalous hydrocarbon activity of the Ag foam.[7]

Fig. 4 summarizes possible mechanistic pathways of the CO_2 conversion on the improved Ag foam catalyst.[7] The experimentally observed hydrocarbon formation clearly indicates that the novel Ag foam shares, at least in parts, essential electrocatalytic properties with Cu-based catalysts.

Not only are the general electrocatalytic activity and product selectivity important for the overall performance evaluation of the catalyst but also its stability under reactive conditions. Fig. 5 demonstrates a notable stability of the Ag foam catalyst during CO production at –0.8 V vs RHE. Gaseous products were analyzed in intervals of 30 min. for an electrolysis time of 72 h. Only a minor catalyst deactivation can be deduced from the FE_{CO} values, which fall from initial 98% to final 90% during the 72h electrolysis, whereas the anti-correlated FE_{H_2} values rise from 2% to 10%.

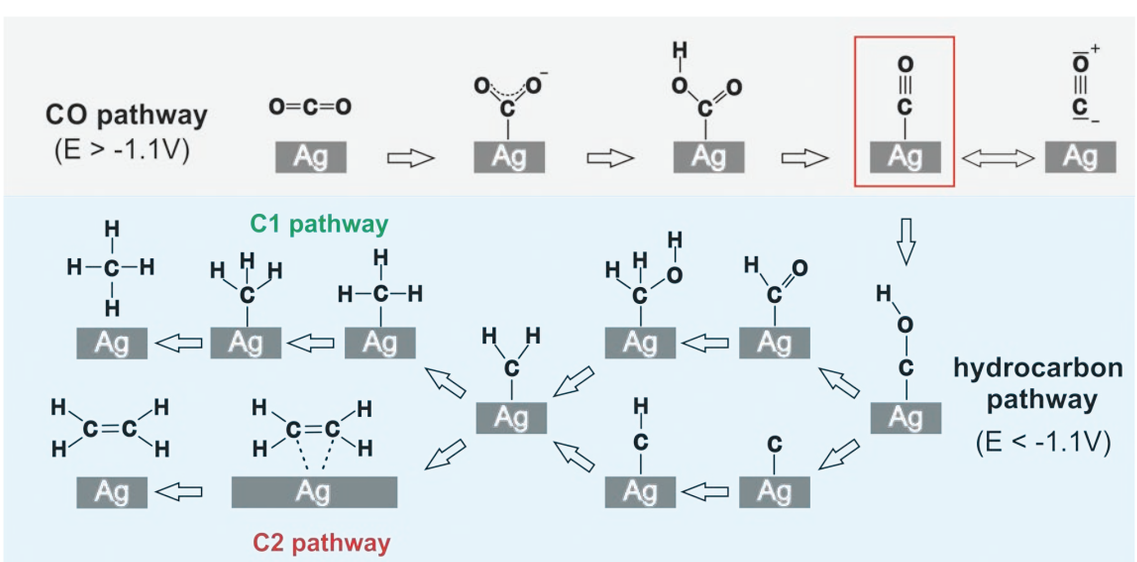

Fig. 4. Scheme demonstrating the mechanistic pathways of CO (panel a) and hydrocarbon formation (panel b) on the novel Ag foam catalyst (reproduced from ref. [7] with permission from the ACS).

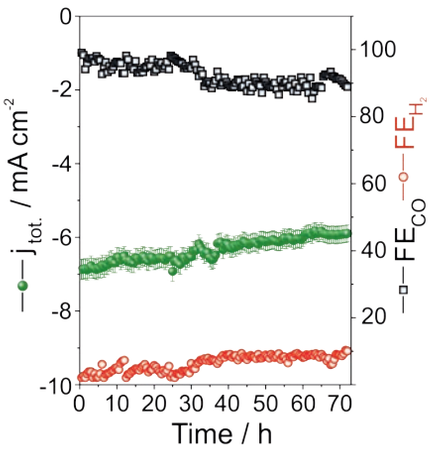

Fig. 5. Long-term stability of the Ag foam catalyst at –0.8 V vs RHE.

2.3 *Preparation and Characterization of Ir-based OER Catalyst*

The development of OER catalysts for electrolysis requires the use of reliable and flexible methods for both catalyst synthesis and optimization as well as activity and stability testing.[12] Fig. 6 depicts the novel Co4Cat technology for the preparation of unsupported and supported precious metal catalysts used in our research group for preparing Ir-based OER catalysts.[13] The technology was developed in the Arenz group in collaboration with the group of S. Kunz at University of Bremen. In the first step of the synthesis, colloidal Ir nanoparticles (NPs) are prepared by heat treatment in alkaline low-boiling point solvents, *e.g.* methanol (MeOH) or ethanol (EtOH) without the addition of any surfactants.

The standard synthesis protocol consists of mixing 6 mL of a 20 mM solution of $IrCl_3$ (Sigma Aldrich, > 99.8 %) in methanol (HPLC grade, Sigma Aldrich) with 21 mL of a 57 mM solution of NaOH (Suprapur®, Merck) in methanol to form a reaction mixture with 4.4 mM of $IrCl_3$ and 44.0 mM of NaOH. Heating the mixture in a 100 mL round bottom flask connected to a water-cooled condenser in a microwave reactor (CEM, Discover SP) for 30 min at power of 100 W leads to the formation of colloidal Ir NPs as indicated by a colour change from 'greenish' to dark brown. The colloidal NPs are extremely stable towards particle agglomeration and can be stored for several months without observing particle sedimentation or agglomeration. As compared to conventional colloidal synthesis approaches using either high boiling point solvents such as ethylene glycol (EG, polyol method)[14] and/or adding surfactants such as polyvinylpyrrolidone (PVP) to the solvent,[15] neither particle precipitation to remove the solvent, nor treatments to remove the surfactant, (*e.g.* ozone treatment or photonic curing[16]) are required. Instead the colloidal Ir NPs can be applied as OER catalyst by spray coating them directly onto an electrode followed by an activation procedure to form IrO_2. Fig. 7 summarizes the results from such a physical and electrochemical characterization. Characterization of the as-prepared Ir NPs by high-resolution transmission electron microscopy (HRTEM; JEOL 3000F operated at 300 kV equipped with a field-emission gun) demonstrates that the particles are highly dispersed and exhibit a particle size of around 1.6 ±0.3 nm. Electrodes were prepared by pipetting different amounts of Ir NPs onto a glassy carbon (GC) electrode of a rotating disk electrode (RDE). The electrochemical measurements were carried out as reported in a previous work[13a] using a tilted RDE to avoid the trapping of oxygen bubbles. The electrolyte was 0.1 M $HClO_4$ and the effective solution resistance was adjusted to *ca.* 3 Ω by an analogue feedback scheme[17] of the potentiostat (NordicElectrochemistry ECi-200). Before the activation of the Ir NPs their electrochemically active surface area (ECSA) was determined *via* CO stripping, *i.e.* holding the electrode potential at 0.15 V_{RHE} in a CO-saturated electrolyte, subsequent CO removal by purging with Ar, and oxidation of the adsorbed CO monolayer to CO_2 by scanning the potential from 0.15 V_{RHE} to 1.4 V_{RHE} at 20 mVs^{-1}. It was found that this surface area determination widely used for Pt-based fuel cell catalysts[14c] is also reliable for determining the ECSA of Ir NPs as long as the Ir can be fully reduced to its metallic state. Although the Ir NPs contain (surface) oxide after preparation with the Co4Cat technology, they can be fully reduced electrochemically. By comparison, electrochemical activation leads to an irreversible IrO_2 phase, which is active for the OER, but does not adsorb CO. Furthermore, it is important to separate the activation procedure from the determination of the OER activity. Otherwise, the OER activity is overestimated due to an overlap of Ir oxidation currents and the catalytic oxygen evolution (OER) currents. Therefore, the Ir activation was performed prior to the OER measurements in a potentiostatic mode by holding the electrode potential for 300 s at 1.6 V_{RHE}. Thereafter the OER performance was evaluated by switching the electrode potential back to 1.20 V_{RHE} and recording an anodic scan to 1.55 V_{RHE} at 10 mV s^{-1} rotating the electrode at 3600 rpm. Defining the current density recorded at 1.5 V_{RHE} as the OER activity of the activated Ir NPs, the specific activity (SA) is independent of the particle density reaching values of around 125 μA cm^{-2}_{Ir}, whereas the mass activity (MA) scales with the ECSA achieving a maximum of about 200 A g^{-1}_{Ir} (Fig. 8), which is substantially higher than reported values for IrO_2-based catalysts.[18] In addition, benchmarking a commercial Ir black sample (not shown) in the same way, lead to a MA of only 50 A g^{-1}_{Ir}.

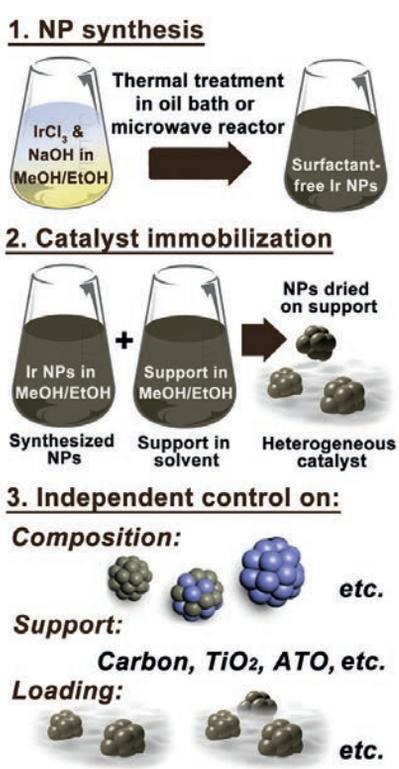

Fig. 6. Scheme illustrating the Co4Cat technology applied for the preparation of Ir-based OER catalysts.

Interestingly, the ECSA and thus the MA exhibits a "volcano-shape" behaviour when plotted as function of particle density on the GC electrode. The decrease towards high density is clearly related to particle agglomeration and the formation of a 3D catalyst layer (also particle agglomeration towards low particle densities is suspected due to the drying process, but this is not proven). The decrease in MA due to agglomeration points towards the main limitation of state-of-the-art Ir-based OER catalysts, *i.e.* their low

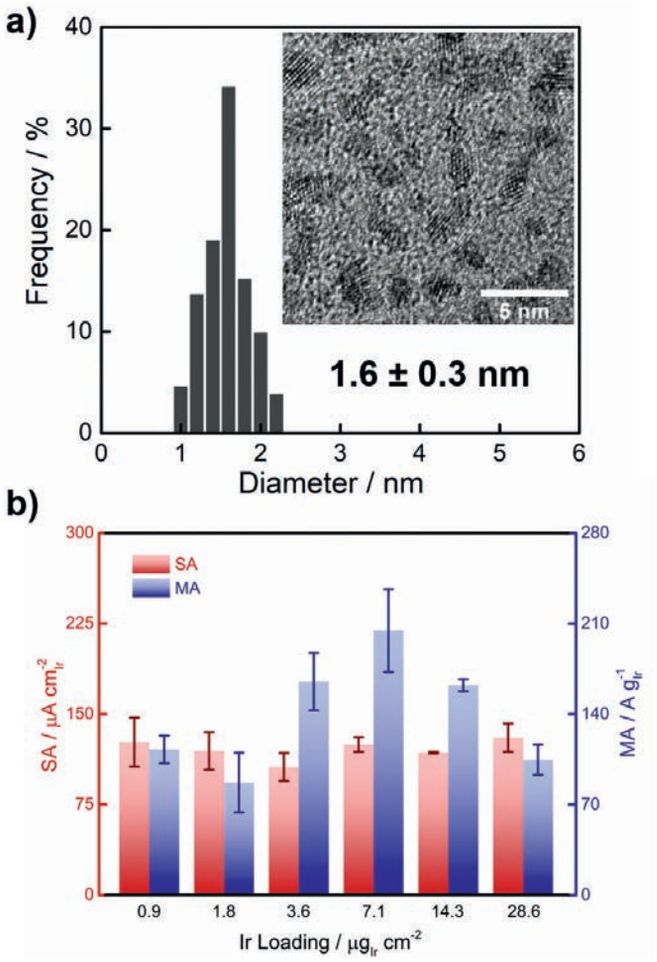

Fig. 7. Particle size distribution histogram of the as-prepared colloidal Ir NPs determined from TEM micrographs. The insert displays a HRTEM micrograph of the Ir NPs; b) specific activity (SA) and mass activity (MA) of activated IrO_2 NPs as a function of their loading on a glassy carbon electrode. All experiments were performed at room temperature. MA and SA were determined at 1.5 V_{RHE} during a positive going potential scan of 10 mV s^{-1}.

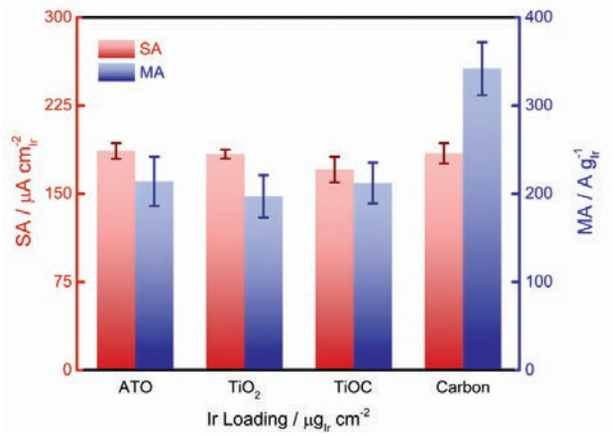

Fig. 8. Specific activity (SA) and mass activity (MA) of supported 50 wt.% Ir-based catalysts. Colloidal Ir NPs have been supported on antimony-doped tin oxide (ATO), TiO2, titanium oxycarbide (TiOC) and Vulcan XC72R (carbon). The Ir loading on the RDE tip was 10 μg$_{Ir}$ cm$^{-2}_{geo}$ for all samples. All experiments were performed at room temperature. MA and SA were determined at 1.5 V_{RHE} during a positive going potential scan of 10 mV s^{-1}.

Ir utilization.[13a] In the field of fuel cell catalysts for the oxygen reduction reaction (ORR) the utilization of Pt could be significantly improved when going from Pt black to carbon-supported Pt catalysts.[19] At the same time, however, carbon corrosion becomes a challenge.[20] For OER catalysts, identifying suitable support materials is even more difficult due to the high electrode potentials required.

One of the advantages of the Co4Cat technology is that the colloidal NPs can also be immobilized onto various support types in a second preparation step (Fig. 6). For this, a suitable support material is mixed in an appropriate low boiling point solvent and combined under stirring with the colloidal Ir NPs. The NPs are immobilized on the support by completely removing the solvents in a rotary evaporator under mild vacuum (10 mbar). The Co4Cat technology has also been proven flexible for varying NP composition, however, for OER these parameters have not yet been fully exploited.

Fig. 8 summarizes a comparison of the SA and MA of the Ir NPs when immobilized onto different supports powders, *i.e.* antimony-doped tin oxide (ATO), TiO_2, titanium oxycarbide (TiOC) and Vulcan XC72R (carbon black). The nominal Ir metal loading on the respective supports was adjusted to 50 wt.%. Interestingly, the observed specific OER activity was independent of the support type, however, higher than the one observed for the unsupported Ir NPs; *i.e. ca.* 175 vs. *ca.* 125 μA cm$^{-2}_{Ir}$ (the activation and activity determination were performed in the same manner as described above). This is surprising and currently it is not certain if the observed differences are a consequence of a 3D vs. 2D catalyst layer. A strong metal support interaction, however, seems unlikely as the support types are quite different.

But not only the SA is improved in comparison to the 2D films, also the MA. Furthermore, the MA of the Ir NPs immobilized on carbon is significantly higher than on the other supports (*ca.* 330 vs *ca.* 220 A g^{-1}_{Ir}). Determination of the ECSAs of the different samples (not shown) reveals that this is directly related to the higher ECSA. As all Ir NPs came from the same batch, the observed differences must be related to either a loss of particles in the immobilization process, different particle agglomeration on the supports, or a limited conductivity. More investigations area required to distinguish between the two explanations. In any case, the results clearly demonstrate that the highly dispersed Ir NPs prepared by the Co4Cat technology can significantly improve the utilization of the precious Ir metal by immobilization onto a proper support material.

3. Conclusions

Herein we discuss recent activities at the Department of Chemistry and Biochemistry at University of Bern concerning the electrochemical water/CO_2 co-electrolysis.

In the first part, we have demonstrated that an additive-assisted metal foam deposition can be considered as a valuable alternative approach to classical colloid chemistry to produce highly selective electro-catalysts for the reductive conversion of CO_2 into CO. The obtained Ag foams show a superior activity and selectivity towards CO production at particularly low and moderate overpotentials. Not only is the onset potential for CO formation of ~ –0.3 V vs RHE considerably lower but also the resulting CO efficiencies never fall below 90% within an extraordinarily broad potential window of ~900 mV ranging from –0.3 V to –1.2 V vs RHE. Most intriguing is the capability of the novel Ag foam catalyst to produce hydrocarbons in significant amounts, reaching CH_4 and C_{2H_4} efficiencies of FE_{CH_4} = 51% and $FE_{C_2H_4}$ = 8.6%, respectively, at –1.5 V vs RHE. This remarkable Cu-like behavior has been rationalized in terms of the *CO binding energy which is significantly increased on the novel Ag foam with respect to polycrystalline Ag foil references.

A key structural feature of the novel Ag foam catalyst is the particular meso-porosity with pore sidewalls that are composed of highly anisotropic, needle-shaped Ag features having dimensions in the nanometer (nm) range. This particular morphology is

obtained only by means of the citrate plating additive controlling the Ag growth on the nm-scale. This work also demonstrates that the tailored design of ec-CO_2RR catalysts can transform a predominantly CO producing catalyst, *e.g.* Ag, into a Cu-like catalyst being capable of producing hydrocarbons.

In the second part, the activities concerning the other half-cell reaction, the OER, are summarized. It is demonstrated that the developed Co4Cat technology allows the preparation and easy handling of highly active OER catalysts, both in unsupported and supported catalysts. The as-prepared Ir NPs can be analysed with respect to their ECSA, SA and MA. This allows a distinction between different mechanisms of activity optimization. It is shown that a simple physical optimization of the dispersion leads to significantly more active OER catalysts with respect to the amount of Ir used (MA). The main challenge is to identify proper support materials that are both highly conducting and stable. While on carbon black the highest utilization and MA is achieved, it is expected that such an OER catalyst will not be stable under continuous electrolysis conditions. Nevertheless, a complete coverage of the support with Ir NPs, as achieved for Pt-based fuel cell catalysts,[21] might shift the electrochemical properties towards IrO_2 black and thus alleviate support corrosion.

Acknowledgement

The financial support by the CTI Swiss Competence Center for Energy Research (SCCER Heat and Electricity Storage) is gratefully acknowledged. P.B. and M.A. acknowledge the financial support by the Swiss National Science Foundation (SNSF) via the project No. 200020_172507 (P.B.) and 200021_184742 (M.A.). J.Q. has received funding from the European Union's Horizon 2020 research and innovation program under the Marie Skłodowska-Curie grant agreement No 703366 (SELECTRON). The group of M.A. acknowledges the collaboration with Dr. S. Kunz (Co4Cat synthesis) and Prof. L. Theil Kuhn (TEM). L. Kacenauskaite is acknowledged for Fig. 6. This study was performed with the support of the interfaculty Microscopy Imaging Centre (MIC) of the University of Bern.

Received: August 6, 2019

[1] D. T. Whipple, P. J. A. Kenis, *J. Phys. Chem. Lett.* **2010**, *1*, 3451.
[2] a) H. Yang, Z. Xu, M. Fan, R. Gupta, R. B. Slimane, A. E. Bland, I. Wright, *J. Environ. Sci.* **2008**, *20*, 14; b) M. Mikkelsen, M. Jørgensen, F. C. Krebs, *Energy Environ. Sci.* **2010**, *3*, 43.
[3] T. Haas, R. Krause, R. Weber, M. Demler, G. Schmid, *Nat. Catal.* **2018**, *1*, 32.
[4] K. W. Frese, S. Leach, *J. Electrochem. Soc.* **1985**, *132*, 259.
[5] a) K. P. Kuhl, T. Hatsukade, E. R. Cave, D. N. Abram, J. Kibsgaard, T. F. Jaramillo, *J. Am. Chem. Soc.* **2014**, *136*, 14107; b) M. Rahaman, A. Dutta, A. Zanetti, P. Broekmann, *ACS Catal.* **2017**, *7*, 7946.
[6] H. C. Shin, M. Liu, *Chem. Mater.* **2004**, *16*, 5460.
[7] A. Dutta, C. E. Morstein, M. Rahaman, A. Cedeño López, P. Broekmann, *ACS Catal.* **2018**, 8357.
[8] A. Dutta, M. Rahaman, N. C. Luedi, M. Mohos, P. Broekmann, *ACS Catal.* **2016**, *6*, 3804.
[9] Q. Lu, J. Rosen, Y. Zhou, G. S. Hutchings, Y. C. Kimmel, J. G. Chen, F. Jiao, *Nat. Commun.* **2014**, *5*, 3242.
[10] Y. Hori, in 'Modern Aspects of Electrochemistry', Springer, New York, **2008**, p. 89, DOI: 10.1007/978-0387-49489-0_3.
[11] T. Hatsukade, K. P. Kuhl, E. R. Cave, D. N. Abram, T. F. Jaramillo, *Phys. Chem. Chem. Phys.* **2014**, *16*, 13814.
[12] H. A. El-Sayed, A. Weiß, L. F. Olbrich, G. P. Putro, H. A. Gasteiger, *J. Electrochem. Soc.* **2019**, *166*, F458.
[13] a) J. Quinson, S. Neumann, T. Wannmacher, L. Kacenauskaite, M. Inaba, J. Bucher, F. Bizzotto, S. B. Simonsen, L. T. Kuhn, D. Bujak, A. Zana, M. Arenz, S. Kunz, *Angew. Chem. Int. Ed.* **2018**, *57*, 12338; b) J. Quinson, L. Kacenauskaite, J. Bucher, S. B. Simonsen, L. T. Kuhn, M. Oezaslan, S. Kunz, M. Arenz, *ChemSusChem* **2019**, *12*, 1229.
[14] a) Y. Wang, J. W. Ren, K. Deng, L. L. Gui, Y. Q. Tang, *Chem. Mater.* **2000**, *12*, 1622; b) J. Quinson, M. Inaba, S. Neumann, A. A. Swane, J. Bucher, S. B. Simonsen, L. T. Kuhn, J. J. K. Kirkensgaard, K. M. O. Jensen, M. Oezaslan, S. Kunz, M. Arenz, *ACS Catal.* **2018**, *8*, 6627; c) M. Inaba, J. Quinson, J. R. Bucher, M. Arenz, *J. Vis. Exp.* **2018**, *133*, e571105.
[15] a) C.-W. Chen, D. Tano, M. Akashi, *J. Coll. Interf. Sci.* **2000**, *225*, 349; b) F. Fiévet, S. Ammar-Merah, R. Brayner, F. Chau, M. Giraud, F. Mammeri, J. Peron, J. Y. Piquemal, L. Sicard, G. Viau, *Chem. Soc. Rev.* **2018**, *47*, 5187.
[16] L. D. Menard, F. Xu, R. G. Nuzzo, J. C. Yang, *J. Catal.* **2006**, *243*, 64.
[17] G. K. H. Wiberg, PhD thesis, **2010**, *http://mediatum.ub.tum.de?id=993285*.
[18] a) H.-S. Oh, H. N. Nong, T. Reier, M. Gliech, P. Strasser, *Chem. Sci.* **2015**, *6*, 3321; b) E. Oakton, D. Lebedev, M. Povia, D. F. Abbott, E. Fabbri, A. Fedorov, M. Nachtegaal, C. Copéret, T. J. Schmidt, *ACS. Catal.* **2017**, *7*, 2346; c) S. M. Alia, B. Rasimick, C. Ngo, K. C. Neyerlin, S. S. Kocha, S. Pylypenko, H. Xu, B. S. Pivovar, *J. Electrochem. Soc.* **2016**, *163*, F3105.
[19] M. S. Wilson, S. Gottesfeld, *J. Appl. Electrochem.* **1992**, *22*, 1.
[20] a) S. J. Ashton, M. Arenz, *Electrochem. Commun.* **2011**, *13*, 1473; b) M. Arenz, A. Zana, *Nano Energy* **2016**, *29*, 299.
[21] J. Speder, A. Zana, I. Spanos, J. J. K. Kirkensgaard, K. Mortensen, M. Hanzlik, M. Arenz, *J. Power Sources* **2014**, *261*, 14.